JOURNAL OF SPACECRAFT AND ROCKETS
Vol. 43, No. 2, March–April 2006

Guidance and Control Design for Hazard Avoidance and Safe Landing on Mars

Edward C. Wong* and Gurkirpal Singh†
Jet Propulsion Laboratory, California Institute of Technology, Pasadena, California 91101
and
James P. Masciarelli‡
NASA Johnson Space Center, Houston, Texas 77058

To ensure successful future Mars landing missions, the lander must be capable of detecting hazards in the nominal landing zone and maneuvering to a new and safe site. Trajectory guidance and attitude commanding are formulated for the terminal descent phase when the lander is off the parachute. The autonomous six-degree-of-freedom controls are accomplished using engines and thrusters and guided by onboard hazard-avoidance sensors. The algorithms determine the available landing zone, survey them for hazards, select the best or alternate landing site based on state estimates and available propellant, and then maneuver the lander to land safely at the selected site. Computer simulations have demonstrated the satisfactory performance of the algorithms for safe landing on Mars with assumed atmospheric environments.

Nomenclature

a	=	acceleration
a_t	=	target acceleration
a_v	=	desired vertical acceleration at landing
C_0, C_1, C_2	=	coefficients of acceleration profile
g	=	acceleration caused by gravity (at Mars)
h	=	height of vertical phase
m	=	mass at start of powered descent
m_{prop}	=	mass of propellant for landing
q	=	attitude quaternion
r	=	position relative to landing site
r_t	=	target position
r_0	=	initial position
t_{go}	=	time to go until reaching target
$t*$	=	time at velocity extreme point
$\mathcal{V}\{.\}$	=	vector part of the quaternion argument
v	=	velocity relative to landing site
v_{exhaust}	=	propulsion system exhaust velocity
v_t	=	target velocity
v_{td}	=	desired vertical velocity at landing
v_0	=	initial velocity
$v*$	=	velocity extreme point (minimum or maximum)
y	=	horizontal landing coordinate position
z	=	horizontal landing coordinate position
ΔV	=	ideal change in velocity
ΔV_x	=	vertical component of ideal change in velocity
ΔV_y	=	horizontal component of ideal change in velocity
ΔV_z	=	horizontal component of ideal change in velocity
$\otimes$	=	quaternion multiplication operator

Introduction

AUTONOMOUS safe landing is an important capability required to ensure mission success for future Mars landing missions. Previous landers, such as the Mars Pathfinder lander, had no closed-loop sensory feedback on hazards (e.g., surface roughness and slope) in the potential landing area.[1] Future landing missions will target scientifically interesting features that lie in areas far more hazardous than those attempted by previous landers. For these sites, hazard avoidance during landing cannot rely solely on rock abundance statistics derived from on-orbit observations at currently available resolutions. To avoid hazards and land safely, future landers must be capable of detecting hazards in the landing zone, designating a safe landing site, and maneuvering to the selected safe site. This requires autonomous, onboard trajectory and attitude planning and execution, with hazard detection sensors in the control loop.

A typical Mars entry vehicle consists of a lander with payload, an aeroshell, and a parachute. During atmospheric entry, the lander is contained within the aeroshell, which protects the lander from aerodynamic loads and heating as the vehicle enters the atmosphere at high velocity and decelerates. When aerodynamic loads and heating are small and the entry vehicle has descended to an appropriate altitude and velocity, a parachute is deployed to further slow the vehicle. The aeroshell is then separated, and the parachute extracts the lander from the aeroshell. Subsequently the parachute turns the lander's flight path so that it is falling nearly vertically at a terminal velocity of about 50 m/s. When the lander reaches 500–1000-m altitude, the parachute is jettisoned, and the lander uses its propulsion system to perform final maneuvers and land safely on the surface of Mars.

Prior work in autonomous guidance for the Apollo lunar module was done for the moon missions.[2] The autonomous guidance and control (G&C) design under consideration here for Mars landing consists of onboard capabilities for the terminal descent phase of flight, which starts once the parachute is deployed and ends at touchdown on the surface. During terminal descent, the vehicle must determine its position, velocity, and attitude; determine the available landing zone; generate terrain maps; survey them for hazards; select the best landing site; and maneuver to land safely at the selected site. The entire system must operate autonomously. The landing scenario currently being considered is shown in Fig. 1.

This paper will focus on the algorithm design for the trajectory guidance, landing-area prediction, attitude commanding, and the six-degree-of-freedom control of the landing vehicle with proper thruster selection logic. The navigation system used to estimate position, velocity, and attitude is discussed in Ref. 3. The navigation system used for terminal descent is also used during the atmospheric entry phase of flight. The guidance system used during the entry phase is discussed in Ref. 4 and the entry controller in Ref. 5.

Received 4 February 2003; revision received 1 August 2004; accepted for publication 1 February 2005.

*Principal Engineer, Autonomy and Control Section. Member AIAA.
†Senior Engineer, Autonomy and Control Section.
‡Aerospace Engineer, Aeroscience and Flight Mechanics Division; currently Systems Engineer, Ball Aerospace and Technologies Corporation, Boulder, CO 80301. Senior Member AIAA.

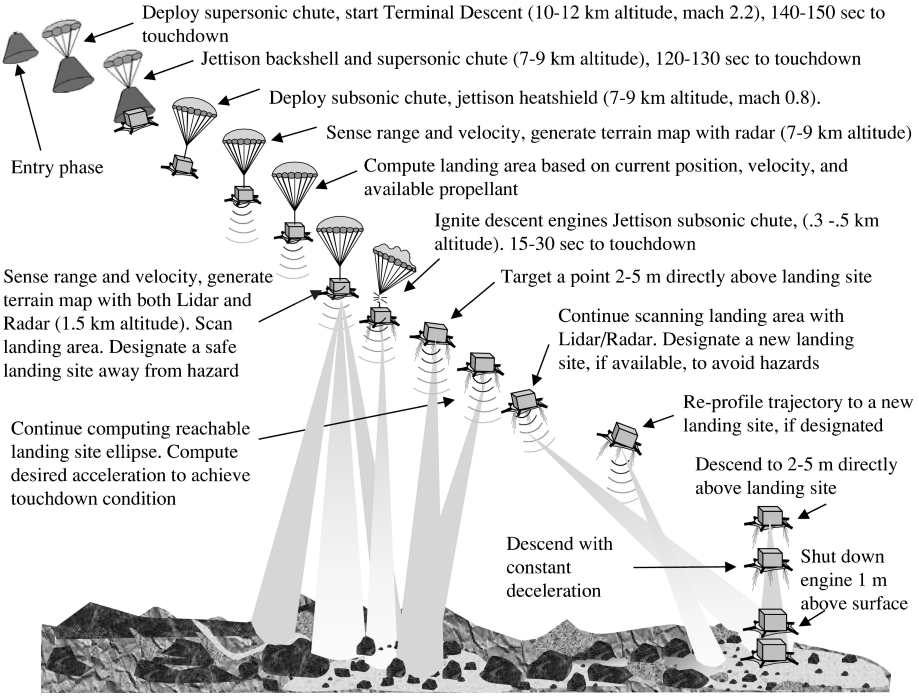

Fig. 1 Representative landing scenario.

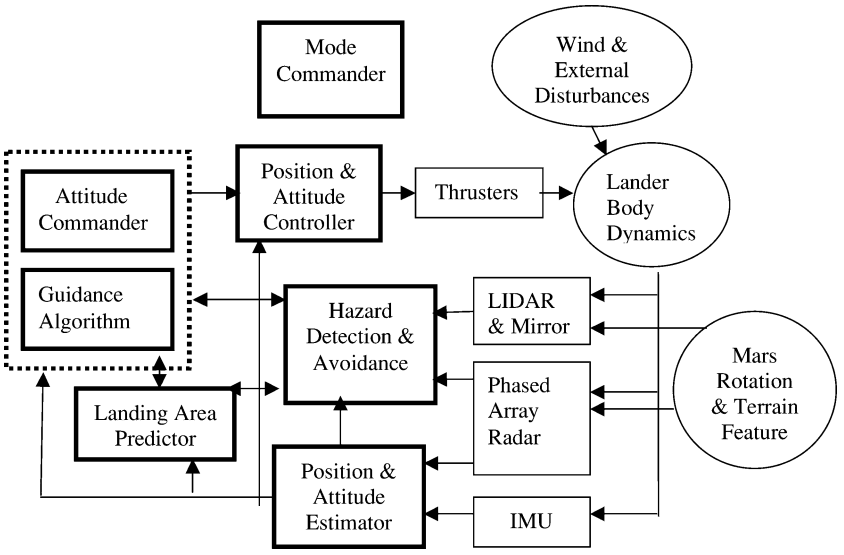

Fig. 2 Guidance and control functions.

Design Approach

The onboard G&C system for powered descent consists of trajectory guidance; attitude commanding; landing vehicle control; landing-area prediction; terrain map generation; hazard detection; landing site selection; and lander position, velocity, and attitude estimation. Figure 2 depicts the G&C functional block diagram. The landing-area predictor establishes the appropriate landing zone. The hazard detection and avoidance system scans the landing zone and then identifies a safe landing target. The trajectory guidance and attitude commander provides commands to steer the vehicle to the selected landing target, and the position and attitude controller ensures accurate execution of those commands. The navigation system provides estimates of the vehicle's position, velocity, and attitude. Sensors and actuators for landing consists of laser radar (lidar), phased-array radar, inertial measurement unit, and descent engines and roll-control thrusters.

Trajectory Guidance Algorithms

The trajectory guidance system must provide attitude and thrust commands to guide the lander from some initial position, velocity, attitude, and angular rate to a specified target position, velocity, attitude, and angular rate. The target position can be changed a number of times during the terminal descent as hazards are detected, and the guidance system must be able to adjust to the new targets. In addition, the guidance system must determine the potential landing area based on the available propellant and issue the command to terminate parachute flight and begin the powered descent.

The guidance algorithm described here is similar to that used for the Apollo lunar module,[2] except that modifications have been made for the specific Mars landing requirements and to enable prediction of the available landing zone. The guidance equations are developed in a coordinate frame that is fixed with respect to the rotating planet surface. Thus it is assumed that the current position and velocity

vectors, as well as the target position and velocity vectors, are given in the surface-fixed frame. The output from the trajectory guidance system is an instantaneous acceleration vector, in the surface-fixed frame, that must be provided by the vehicle's control system to fly to the given target conditions.

Computing the Acceleration Profile

We seek an acceleration profile $a(t)$ that passes through the initial state and the target state. Once this has been found, the thrust magnitude and direction are adjusted to produce the desired acceleration profile. Note that target acceleration and velocity vectors control the target attitude. For example, if horizontal velocities and accelerations are equal to zero, the vehicle will be in an erect attitude. Therefore, we need to solve a two-point boundary-value problem, where the boundary conditions are the initial position and velocity r_0, v_0, and the target position, velocity, and acceleration r_t, v_t, a_t. Because our target state specifies three constraints (position, velocity, acceleration), we select a quadratic acceleration profile of the form

$$a(t) = C_0 + C_1 t + C_2 t^2 \tag{1}$$

where C_0, C_1, and C_2 are coefficients to be determined. Then, by integration, it follows that the velocity and position are given by

$$v(t) = C_0 t + (1/2)C_1 t^2 + (1/3)C_2 t^3 + v_0 \tag{2}$$

$$r(t) = (1/2)C_0 t^2 + (1/6)C_1 t^3 + (1/12)C_2 t^4 + v_0 t + r_0 \tag{3}$$

Let t_{go} denote the time elapsed in traveling from our current state to the target state. We can then use Eqs. (1–3) to write

$$a_t = C_0 + C_1 t_{go} + C_2 t_{go}^2 \tag{4}$$

$$v_t = C_0 t_{go} + (1/2)C_1 t_{go}^2 + (1/3)C_2 t_{go}^3 + v_0 \tag{5}$$

$$r_t = (1/2)C_0 t_{go}^2 + (1/6)C_1 t_{go}^3 + (1/12)C_2 t_{go}^4 + v_0 t_{go} + r_0 \tag{6}$$

which can be solved to provide the desired coefficients:

$$C_0 = a_t - 6[(v_t + v_0)/t_{go}] + 12\left[(r_t - r_0)/t_{go}^2\right] \tag{7}$$

$$C_1 = -6(a_t/t_{go}) + 6\left[(5v_t + 3v_0)/t_{go}^2\right] - 48\left[(r_t - r_0)/t_{go}^3\right] \tag{8}$$

$$C_2 = 6\left(a_t/t_{go}^2\right) - 12\left[(2v_t + v_0)/t_{go}^3\right] + 36\left[(r_t - r_0)/t_{go}^4\right] \tag{9}$$

With these coefficients, the vehicle's position, velocity, and acceleration as a function of time are now determined for one axis. The process is carried out for each coordinate axis (two horizontal, one vertical) to obtain the position, velocity, and acceleration vectors. Note that we must subtract the acceleration vector caused by gravity from the total desired acceleration to get the acceleration vector that must be provided by the vehicle's thrust. We recompute C_0, C_1, and C_2 each guidance cycle, reducing t_{go} as we approach the target. Note that we must divide by powers of t_{go} in Eqs. (1–9). This presents a problem as the vehicle approaches the target state and the transfer time approaches zero.

The solution to this problem is to not recompute C_0, C_1, and C_2 when t_{go} gets small. Let t_{epoch} denote the last time that the values for C_0, C_1, and C_2 were computed, and let t denote the current time. When t_{go} becomes small, the desired acceleration is computed by

$$a = C_0 + C_1(t - t_{epoch}) + C_2(t - t_{epoch})^2 \tag{10}$$

If the control system perfectly executes the commanded acceleration profile, then this approach will deliver the vehicle exactly to the target state. In reality, however, some accuracy will be lost because of external disturbances. The loss in accuracy is proportional to the length of time that the acceleration profile coefficients are not recomputed (fine count time). Thus there is a tradeoff between stability in computing the acceleration polynomial coefficients and landing accuracy. Our trajectory simulation results show sufficient numerical stability and negligible loss in landing accuracy for a fine count time of 2 s.

Computing Transfer Time

The acceleration profile just developed did not assume any particular value for the transfer time t_{go}. To compute a transfer time, we can select t_{go} such that the vertical component of the acceleration profile is a linear function of time. This is equivalent to imposing the additional constraint of $C_2 = 0$ for only the set of equations in the vertical direction. (C_2 remains nonzero in the two sets of equations for the two horizontal directions.) Then, for the vertical direction only, we can write

$$a_t = C_0 + C_1 t_{go} \tag{11}$$

$$v_t = v_0 + C_0 t_{go} + \tfrac{1}{2}C_1 t_{go}^2 \tag{12}$$

$$r_t = r_0 + v_0 t_{go} + \tfrac{1}{2}C_0 t_{go}^2 + \tfrac{1}{6}C_1 t_{go}^3 \tag{13}$$

which are three equations for the three unknowns C_0, C_1, and t_{go}. Solving for t_{go}, we find that if a_t is not zero,

$$t_{go} = (2v_t + v_0)/a_t + \sqrt{[(2v_t + v_0)/a_t]^2 + 6(r_0 - r_t)/a_t} \tag{14}$$

If $a_t = 0$ (constant vertical velocity), the solution for t_{go} is

$$t_{go} = 3(r_t - r_0)/(v_0 + 2v_t) \tag{15}$$

Guidance Targets

The lander can be made to follow a general trajectory shape by flying to one or more intermediate targets or waypoints. Currently, we use one intermediate waypoint resulting in the following two trajectory segments: the approach phase, in which the lander flies to a point directly above the intended landing site, and the vertical phase, in which the lander descends with constant acceleration to the landing site. This trajectory requires one set of targets for the end of the approach phase and the second set for the end of the vertical phase.

The vertical component of velocity required at the beginning of the vertical phase (end of approach phase) is computed from kinematics. Horizontal components of velocity and acceleration are zero to make the vehicle land in an erect attitude. Therefore, given the constant vertical acceleration during the vertical phase a_v, the touchdown velocity v_{td}, the height of the vertical phase h, and the horizontal landing coordinates y, z, the approach phase targets are

$$\boldsymbol{r}_t = [h \quad y \quad z], \qquad \boldsymbol{v}_t = \left[-\sqrt{v_{td}^2 + 2a_v h} \quad 0 \quad 0\right]$$
$$\boldsymbol{a}_t = [a_v \quad 0 \quad 0] \tag{16}$$

and the vertical phase targets are

$$\boldsymbol{r}_t = [0 \quad y \quad z], \qquad \boldsymbol{v}_t = [v_{td} \quad 0 \quad 0], \qquad \boldsymbol{a}_t = [a_v \quad 0 \quad 0] \tag{17}$$

Parachute Release Command

To determine when to begin powered descent, the guidance system computes the desired thrust acceleration vector during parachute flight assuming that powered descent is to begin at the current instant. The desired thrust magnitude is then computed using the desired thrust acceleration and the mass of the lander. The powered descent phase is initiated when the desired thrust magnitude exceeds a certain value. Otherwise, parachute flight continues. The thrust magnitude value used to trigger parachute release is selected empirically based on Monte Carlo trajectory simulations that take into account expected dispersions. A value of 75 to 90% of the available thrust typically provides a good balance between minimizing propellant consumption and leaving margin to handle dispersions. The process is repeated each guidance cycle until powered flight is initiated. With this logic, powered descent will begin at as low an altitude as possible for the available thrust, thereby minimizing

terminal descent propellant use. This, in addition to the constraint of linear vertical acceleration, also ensures that the lander's trajectory monotonically decreases in altitude and does not pass through the ground to reach the target conditions.

Landing-Area Predictor

The first step in determining the available landing area is to define the nominal landing point. To do this, we make the horizontal components of the acceleration profile linear functions of time instead of quadratic functions of time, that is, set $C_2 = 0$ and use Eqs. (1–3) to solve for the target position r_t at time t_{go}, which results in

$$r_t = -\tfrac{1}{6}a_t t_{\text{go}}^2 + \left(\tfrac{1}{3}v_0 + \tfrac{2}{3}v_t\right)t_{\text{go}} + r_0 \tag{18}$$

Because the target horizontal velocity and acceleration are zero, the horizontal components of the nominal landing point are computed from

$$r_t = r_0 + \tfrac{1}{3}v_0 t_{\text{go}} \tag{19}$$

Given a target landing site, the ideal change in velocity ΔV required to reach that site is

$$\Delta V = \sqrt{\Delta V_x^2 + \Delta V_y^2 + \Delta V_z^2} \tag{20}$$

where

$$\Delta V_x = v_{t_x} - v_{0_x} + g t_{\text{go}}, \qquad \Delta V_y = -v_{0_y} + 2v*_y$$
$$\Delta V_z = -v_{0_z} + 2v*_z \tag{21}$$

and the subscript x denotes the vertical direction and subscripts y and z denote the horizontal directions. If the ideal ΔV is known, the propellant required can be computed using the rocket equation

$$m_{\text{prop}} = m[1 - \exp(-\Delta V / V_{\text{exhaust}})] \tag{22}$$

Therefore, to determine the available landing area, we do a search of landing sites around the nominal site to find the ellipse that fits within the available amount of propellant. Before we can compute the propellant required for landing, we need to determine the values for velocity extreme points $v*$ in Eq. (21).

We know our horizontal velocity profile is given by Eq. (2), and its derivative, the acceleration, from Eq. (1). We let $a(t) = 0$ and solve for the times at which velocity extreme points occur [making use of Eqs. (7–9)]. We find zeros at t_{go} (as expected) and

$$t* = \left(\frac{t_{\text{go}}}{2}\right)\frac{v_0 t_{\text{go}} - 2(r_t - r_0)}{v_0 t_{\text{go}} - 3(r_t - r_0)} \tag{23}$$

If $0 < t* < t_{\text{go}}$, then the vehicle will go through this velocity extreme point. The velocity at the extreme point is given by evaluating Eq. (2) at time $t*$:

$$v* = C_0 t* + \tfrac{1}{2}C_1 t*^2 + \tfrac{1}{3}C_2 t*^3 + v_0 \tag{24}$$

If $t* < 0$ or $t* > t_{\text{go}}$, we set $v* = 0$ in Eq. (21) as appropriate.

Attitude Command and Control Algorithms

The attitude commander generates the attitude command profile for the lander. The controller commands the thrusters and descent engines to follow the commanded attitude profile and guidance-derived acceleration command at a desired control cycle frequency, currently determined to be 10 Hz.

Reference Attitude Command Generation

The commanded attiude is a function primarily of the acceleration commanded by the trajectory guidance algorithm. Trajectory guidance provides an acceleration command in surface relative coordinates. The command is compensated for the Martian gravity and transformed into inertial coordinates before the attitude commander uses it. The desired attitude of the lander must be such that the descent engine thrust direction is aligned with the guidance acceleration command in inertial coordinates. This defines the primary pointing constraint enforced by the attitude commander function. The primary pointing constraint fixes two of the three pointing degrees of freedom. Currently there is no preferred roll orientation for the Mars lander. For this reason we have fixed the roll orientation at the initial value. This limits the roll motion around the engine thrust direction. Let $a_I(t)$ be the total desired linear acceleration in inertial coordinates, p_b be the primary thrust direction in lander coordinates, and s_b be any vector orthogonal to p_b. To fix the roll orientation, we define a fixed inertial vector s_I as the inertial pointing direction of s_b at the start of powered phase:

$$s_I = \mathcal{V}\{\bar{q}_e(0) \otimes s_b \otimes q_e(0)\} \tag{25}$$

where $\bar{q}_e(0)$ is the conjugate of $q_e(0)$, the lander estimated attitude at start, $\otimes$ implies a quaternion multiplication, and $\mathcal{V}\{.\}$ stands for the vector part of the quaternion argument. The desired attitude q_d satisfies the following two pointing constraints:

$$\text{Unit}(a_I) = \mathcal{V}\{\bar{q}_d \otimes p_b \otimes q_d\} \tag{26}$$

$$s_I \approx \mathcal{V}\{\bar{q}_d \otimes s_b \otimes q_d\} \tag{27}$$

The first is the primary pointing constraint, and Eq. (27) is the secondary pointing constraint. The latter cannot be satisfied exactly, in general. Other preferred roll orientations can be enforced simply by choosing an appropriate constraint (27). The desired attitude derivation based on a primary-secondary pointing construct is very similar to the one used in the Cassini attitude and articulation control system. In the sequel we shall refer to the desired attitude as the lander base attitude. The desired base angular rate is derived from the base attitude.

Attitude Profiling

Once the reference attitude of the lander has been computed, the next step is to smoothly bridge the gap between the current attitude and rate and the desired attitude. This process is referred to as attitude profiling here. The intent is to effect a change in lander attitude in a smooth fashion, by commanding an attitude profile, which does not exceed specified rate and acceleration limits. The attitude profiles are defined relative to the lander base attitude. The expectation is that once the initial offset between the base attitude and lander initial attitude has been removed the smoothness of the guidance acceleration command will require no more profiling except, possibly, at the start of the vertical phase. The initial offset in attitude and rate is removed in two steps: a rate matching phase, where the idea is to null the base attitude-relative angular rate, and a position matching phase, which removes the total position offset. At the end of the position matching phase, the vehicle attitude command is exactly aligned with the desired or the base attitude. The lander has large angular acceleration capability about any axis orthogonal to the roll axis. Therefore the offset removal lasts for a very short time. The guidance acceleration command is expected to meet certain smoothness conditions. The attitude commander simply invokes attitude profiling when certain "smoothness" conditions are violated.

Controller and Thruster Selection Logic

Following the processing of the trajectory guidance and attitude commander functions, we have a desired total vehicle acceleration in inertial coordinates and a commanded vehicle attitude (inertial relative) and angular rate. The controller uses these commands to construct the desired force f_b and a torque τ_b on the lander. The

desired force computation is straightforward. The desired force in inertial coordinates is simply the guidance-commanded inertial acceleration times an estimate of the lander mass. The inertial force, transformed to the lander body coordinates through the lander attitude estimate, becomes the desired force command, that is,

$$f_b = \mathcal{V}\{q_e \otimes (Ma_I) \otimes \bar{q}_e\} \tag{28}$$

Note that at the base attitude the force command is entirely along the descent engine thrust direction. The desired torque computation is based on a simple proportional-integral-differential (PID) control logic, where commands are compared with the estimates. The resulting errors are used to compute the desired torque signal, that is,

$$\tau_b = 2k_p \mathcal{V}\{q_c \otimes \bar{q}_e\} + k_d\{\omega_c - \omega_e\} + 2k_i \int \mathcal{V}\{q_c \otimes \bar{q}_e\}\,\mathrm{d}t \tag{29}$$

Here, as is usual in attitude control applications, care is exercised in normalizing the attitude error (the first term), and only the vector part of it is used. The coefficients (the PID gains) are in general constant, 3×3 diagonal matrices. Care is exercised in limiting the attitude, rate, and integral control error terms appropriately before combining them [Eq. (29)]. The integral term has a large enough gain to quickly learn any bias torques on the vehicle (cumulative effects of uncertainties in vehicle center-of-mass location, inertia, thrust vectors, thrust locations, and aerodynamic torques). The proportional and derivative gains are chosen to achieve a proper balance between response and robustness. For a 0.1-s control cycle it is possible to realize a 0.7-Hz attitude control-loop bandwidth with a 7-dB gain and 35-deg phase margins.

We have found enforcement of zero-attitude-control deadband about lateral axes (x, y) to provide better overall performance. Therefore the controller is constantly trying to maintain near-zero x, y attitude and rate control errors. Because on-off thrusters are used exclusively to control attitude motions about the roll z axis, in order to avoid excessive control action about the z axis, a nonzero-attitude-control deadband is prescribed in this axis. The controller-computed desired force and torque commands (both in lander body coordinates) are subsequently fed to the thruster selection logic. The force actuators on the lander are made up of smaller on-off, pulse-width modulated thrusters (eight in the current baseline) and large, throttleable descent engines (six in the present baseline). The thrusters, which are also used during the guided entry phase, provide, primarily, the roll control. The descent engines provide almost all of the needed force and, by virtue of differential throttling, the torques about axes orthogonal to the roll axis.

The on-off thrusters are commanded by specifying an appropriate on-time duration lasting between 0 and 100 ms. The descent engines are commanded by specifying an appropriate throttle setting between 20 and 100%. The minimum command-able throttle setting in the current baseline is 20% until the engines are cut off a few meters above the surface. A single logic drives the entire propulsion subsystem by issuing appropriate thruster on-off commands and descent engine throttle settings. The mathematical formulation treats both types of force devices using an equivalent framework where the descent engines are also treated as equivalent on-off thrusters. The problem of computing appropriate actuator commands for an overdetermined system, often referred to in the literature as the control allocation problem, is posed as a nonlinear programming problem, where the cost function is a weighted combination of fuel consumption, force, and torque residuals (residuals are defined as the difference between the desired and the achieved values). Weights are configuration dependent and are also chosen to enforce convexity on the cost function. Feasibility constraints are imposed on the solution. The constraints are in the form of lower and upper bounds. For thrusters the bounds are simply [0, 0.1] s. For descent engines they are [0.02, 0.1] s. Note the equivalence: the minimum throttle setting of 20% is equivalent to an on-time duration of 0.02 s during a 0.1-s control cycle. The upper bound of 0.1 s implies engines operating at 100% throttle during the entire 0.1-s interval. The solution is in the form of on-time durations. The equivalent on-time solutions for the descent engines are converted into desired throttle settings before transmitting to the propulsion subsystem. The control allocation problem does not have a closed-form solution in general. The solution approach is a gradient-based, iterative steepest descent algorithm. Because the cost function is globally convex, a continuous improvement (i.e., a monotonic reduction in the cost function) guarantee can be offered. To realize a real-time implementation, the logic exits after executing a fixed number of iterations. Iterations on the order of 10 or so are found to be more than adequate for this application. Approximately 5200 floating point operations are required to make a single, 10-iteration pass through the algorithm. The required floating point operations are well within the processing resources allocated to the onboard guidance and control system.

Simulation Results

The results from a nonlinear simulation of the lander guidance, navigation, and control system functioning in the Martian environment are presented next. Lander mass and moments of inertia at the start of the powered descent phase are 1521 kg and {963, 1170, 1382} kg · m^2. There are eight thrusters, each capable of producing 67 N of steady-state thrust. The six descent engines distributed on a circular ring of approximately 1-m radius deliver 3047-N (each) thrust at 100% throttle. For the purposes of applying aerodynamic forces and torques on the vehicle, a cylindrical shape 1.1 m in height and 4.0 m in diameter is assumed. Coefficient of drag is 2.0, and a constant, surface-relative head wind (blowing from right to left in Fig. 3) of 20 m/s is assumed. Further, a uniform air density of 0.023 kg/m^3 is assumed throughout. Worst-case aerodynamics loads during terminal descent in this case are less than 2% of the vehicle maximum thrust and torque capabilities. The aerodynamic forces and torques act as external disturbances on the vehicle, which are easily compensated for through the close-loop control action. Terminal guidance compensates for the position errors induced as a result by recomputing the required acceleration at each step. Attitude control loop compensates for any bias torques induced by aerodynamics through the integral control action. In the surface-fixed coordinate frame, the lander is initially 200 m behind and 500 m above the targeted landing site, moving with a velocity of 20 m/s toward the target while descending at 30 m/s. The vertical phase begins 5 m above the surface and has a constant descent rate of 1 m/s. A target redesignation occurs at 6 s into the powered phase. The redesignation moves the desired touchdown location 100 m closer to the lander in the flight plane.

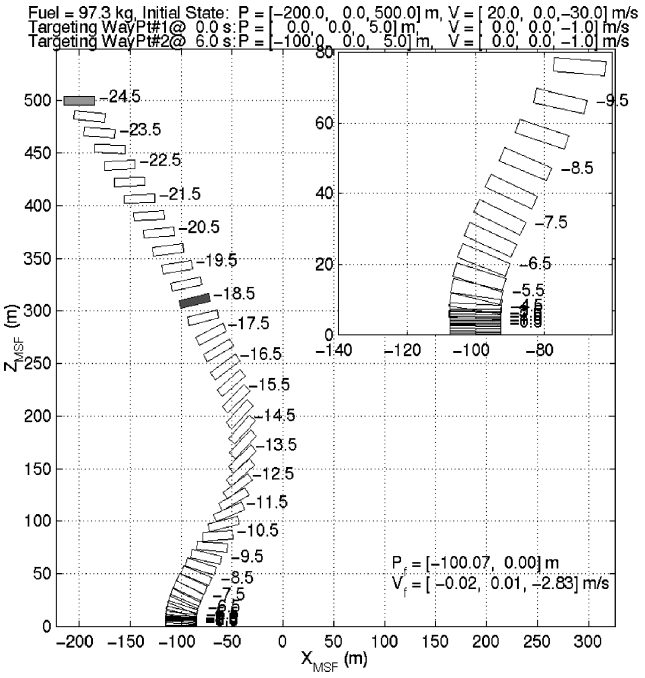

Fig. 3 Powered descent with 100 m divert to new target at 18.5 s to touchdown.

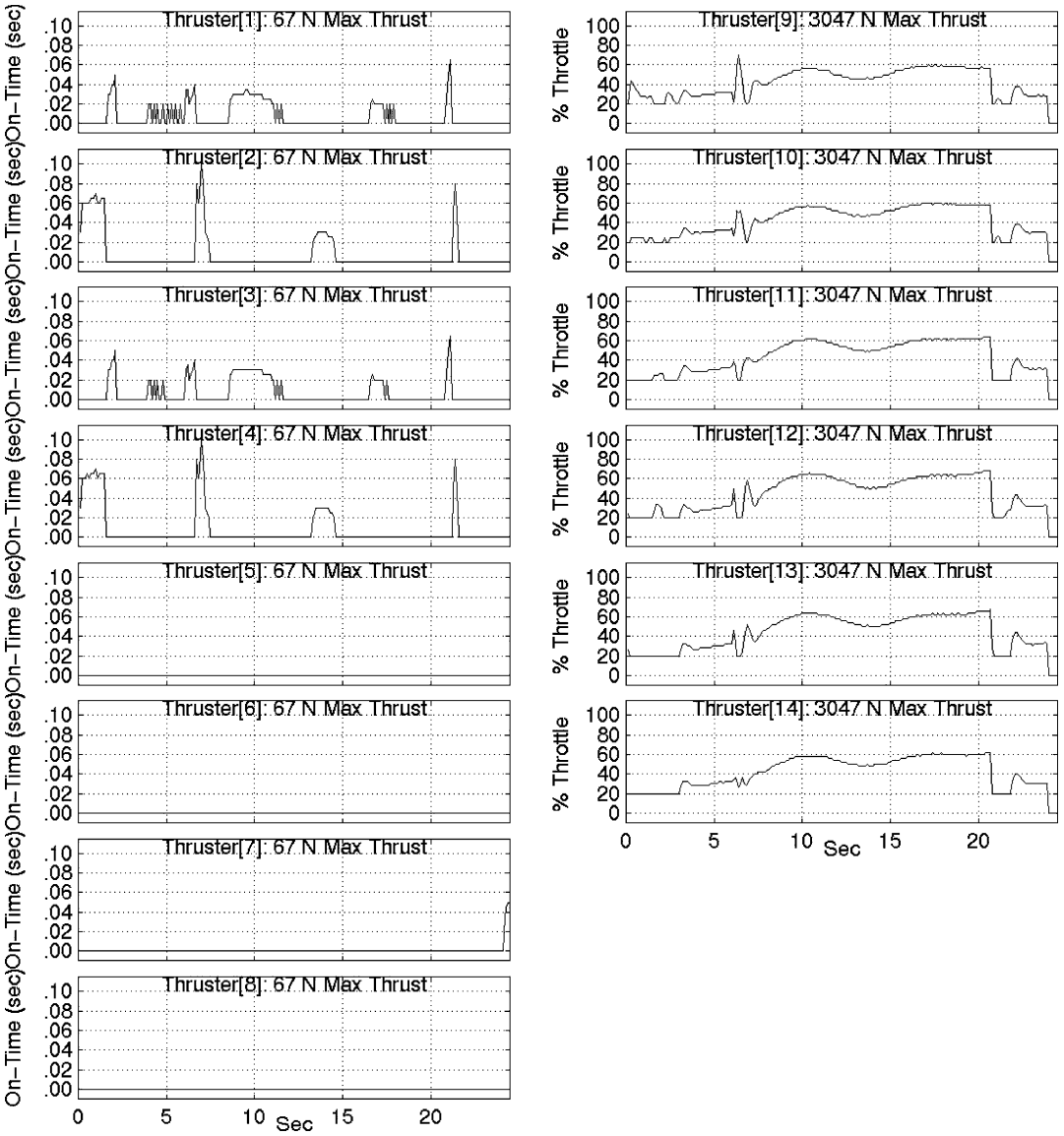

Fig. 4 Commanded thrust and throttle profiles.

Motions in this case are for the most part confined to the initial flight plane. The required attitude motions are either a pitch up or pitch down in this plane. The vehicle motion can therefore be depicted as a box, whose center moves as the lander center of mass in the flight plane (local vertical-local horizontal) and whose orientation is consistent with the lander pitch attitude. The motion of the lander (depicted as an oversized box) at 0.5-s intervals is shown in the surface-fixed local vertical (y axis)–local horizontal (x axis) plane in Fig. 3. Flight lasts for 24.5 s and requires 97.3 kg of fuel. The numbers shown to the right of every other box is the time to go until landing. The initial landing site is located at the origin, the (0, 0) point. The redesignation at 6 s into the flight, at a height of approximately 300 m, places it at $(-100, 0)$ m. The ensuing pitch up and pitch reversal later on are clearly evident. The last 10 s of the flight are magnified in the inset.

The desired thruster commanded on-time durations (on the left), and descent engine throttle settings (right) are shown in Fig. 4. Note the guidance-commanded engine cutoff near the end after which the commanded throttle level falls to zero. Throttle transients in the neighborhood of 6 s are the result of redesignation. Maximum commanded throttle level in this case was less than 70%. The first four (left) thruster on-time durations belong to the thrusters used for roll control. Although no such restriction was imposed in the thruster selection logic, they are the only ones exercised in this simulation.

During the descent simulation, the laser radar terrain sensor field-of-view coverage was analyzed as a function of time. The field of view shrank rapidly during the short 0.5-min terminal descent, which limits the ability to perform more extensive hazard survey and new target selection. The percent time of target site tracking during terminal descent has also been analyzed. It was shown that the terrain sensor could lose track 35% of the time during descent if the sensor were either not aided by an external mirror to increase the effective field of view or such mirror would have only very limited gimbal range.

A preliminary assessment has also been done to predict the lander dynamics in 6-degree of freedom while it was on the parachute and its effect on the terrain sensor field-of-view motion. Such a study also necessitated a preliminary parachute model during descent with assumed Mars environment parameters.

Conclusions

A guidance and control design for automated hazard avoidance and safe landing on Mars has been formulated. The design consists of onboard capabilities for the terminal descent phase that begins when the parachute is deployed and ends at lander touchdown on the surface.

The powered descent guidance algorithm solves a two-point boundary-value problem to guide the vehicle from its current state

to the desired target state. In solving the boundary-value problem, we obtain an estimate of the lander's future position, velocity, and acceleration. We use the acceleration profile to command thrust and attitude. We use the velocity profile to predict propellant consumption. The acceleration profile is linear in the vertical channel and quadratic in the horizontal channels. If the landing coordinates are not specified, we can make the acceleration profile linear in all channels. We can satisfy future additional constraints by increasing the order of the polynomial representing the acceleration profile.

An attitude commander takes the commanded acceleration vector generated by the guidance algorithm and computes attitude and attitude rate commands. The attitude controller then takes these commands and determines an optimum combination of thruster on-off times and throttle settings to achieve the desired commands.

Prototype algorithms are being developed and tested in an integrated six-degree-of-freedom simulation in assumed Mars environments. Computer simulations have demonstrated the performance of the various G&C algorithms. The demonstrated capabilities include powered descent propellant usage, lander divert capability of at least 100 m from initial landing target, and various descents with different initial altitudes and distances behind the designated landing sites. The results have demonstrated that the formulated algorithms can provide adequate hazard avoidance and safe landing of the vehicle on Mars under the assumed Mars atmospheric environment.

Acknowledgments

The design and development described in this paper was carried out by the Jet Propulsion Laboratory, California Institute of Technology, under contract with NASA, and by NASA Johnson Space Center.

References

[1]Golombek, M. P., Cook, R. A., Economou, T., Folkner, W. M., Haldemann, A. F. C., Kallemeyn, P. H., Knudsen, J. M., Manning, R. M., Moore, H. J., Parker, T. J., Rieder, R., Schofield, J. T., Smith, P. H., and Vaughan, R. M., "Overview of the Mars Pathfinder Mission and Assessment of Landing Site Predictions," *Science*, Vol. 278, Dec. 1997, pp. 1743–1748.

[2]Klumpp, A., "Apollo Lunar Descent Guidance," *Automatica*, Vol. 10, No. 2, 1974, pp. 133–146.

[3]Crain, T., and Bishop, R., "Precision Onboard Navigation: Entry Through Landing," AIAA Paper 2002-4501, Aug. 2002.

[4]Mendeck, G., and Carman, G., "Apollo-Derived Entry Guidance for Mars Smart Landers," AIAA Paper 2002-4502, Aug. 2002.

[5]Calhoun, P., and Queen, E., "An Entry Vehicle Control System Design for the Mars Smart Lander," AIAA Paper 2002-4504, Aug. 2002.

M. K. Lockwood
Guest Editor